Euro. Jnl of Applied Mathematics (2000), *vol.* 11, *pp.* 13–28. Printed in the United Kingdom

The asymptotic behaviour of Ramanujan's integral and its application to two-dimensional diffusion-like equations

STEFAN G. LLEWELLYN SMITH[1]

Department of Applied Mathematics and Theoretical Physics, University of Cambridge, Silver Street, Cambridge CB3 9EW, UK
(*email:* sgls1@cam.ac.uk)

(*Received 29 September 1998; revised 21 June 1999*)

The large-time behaviour of a large class of solutions to the two-dimensional linear diffusion equation in situations with radial symmetry is governed by the function known as *Ramanujan's integral*. This is also true when the diffusion coefficient is complex, which corresponds to Schrödinger's equation. We examine the asymptotic expansion of Ramanujan's integral for large values of its argument over the whole complex plane by considering the analytic continuation of Ramanujan's integral to the left half-plane. The resulting expansions are compared to accurate numerical computations of the integral. The large-time behaviour derived from Ramanujan's integral of the solution to the diffusion equation outside a cylinder is not valid far from the domain boundary. A simple method based on matched asymptotic expansions is outlined to calculate the solution at large times and distances: the resulting form of the solution combines the inverse logarithmic decay in time typical of Ramanujan's integral with spatial dependence on the usual similarity variable for the diffusion equation.

1 Introduction

Consider a cylinder of radius $r = a$ whose boundary temperature is raised by an amount V at time $t = 0$, where the evolution of the temperature field, $v(\mathbf{x}, t)$, outside the cylinder is governed by the linear heat equation with diffusivity κ,

$$\frac{\partial v}{\partial t} = \kappa \nabla^2 v. \tag{1.1}$$

This is a classical problem and has been extensively studied in the past. We will consider here the behaviour of the solution for large times, both near the cylinder and far from it.

For simplicity, we keep dimensional variables, although V and κ could be scaled out of the problem if desired. We also set the temperature outside the cylinder at the initial instant to be zero, so v tends to zero for large r. The Laplace transform, denoted by an overbar, is defined by

$$\overline{f}(s) = \int_0^\infty f(t) \mathrm{e}^{-st} \, \mathrm{d}t. \tag{1.2}$$

[1] Present address: Department of Mechanical and Aerospace Engineering, University of California, San Diego, 9500 Gilmon Drive, La Jolle, CA 92093-0411, USA.

The solution to (1.1) in the Laplace variable corresponding to time, which satisfies the boundary condition, is

$$\bar{v} = \frac{VK_0(qr)}{sK_0(qa)}, \tag{1.3}$$

where $q^2 \equiv s/\kappa$ and K_0 is the modified Bessel function of order zero. The solution in the time variable may hence be obtained from the Bromwich integral and has the representation

$$v = V + \frac{2V}{\pi}\int_0^\infty \mathrm{e}^{-\kappa u^2 t}\frac{J_0(ur)Y_0(ua) - Y_0(ur)J_0(ua)}{J_0^2(ua) + Y_0^2(ua)}\frac{\mathrm{d}u}{u}. \tag{1.4}$$

The large-time behaviour of the solution (1.4) is governed by the behaviour of (1.3) near $s = 0$, or equivalently by the behaviour of the integrand in (1.4) near $u = 0$. Near $s = 0$, (1.3) takes the form

$$\bar{v} = \frac{V}{s} - \frac{2V\ln(r/a)}{s\ln(sa^2\mathrm{e}^{2\gamma}/4\kappa)} + O(1), \tag{1.5}$$

where $\gamma = 0.577\ldots$ is Euler's constant. Substituting (1.5) into the Bromwich integral, we obtain

$$v = V + 2V\ln(r/a)N(\tau) + \cdots, \tag{1.6}$$

where the new nondimensional time variable is $\tau \equiv 4\kappa t/a^2\mathrm{e}^{2\gamma}$ and the function N, defined by

$$N(x) \equiv \int_0^\infty \frac{\mathrm{e}^{-ux}}{\pi^2 + (\ln u)^2}\frac{\mathrm{d}u}{u}, \tag{1.7}$$

is known as Ramanujan's integral.

The large-time behaviour of $N(\tau)$ in (1.6) cannot be obtained from a simple use of Watson's lemma due to the singularity of the integrand in (1.7) at the origin. In addition, (1.6) is invalid for large r since it does not decay for large r. This is reflected in the fact that the expansion (1.5) becomes disordered for $qr = O(1)$.

The earliest studies of the problem (1.1), such as Nicholson [1], Goldstein [2], Smith [3], Carslaw & Jaeger [4] and Titchmarsh [5, § 10.10], gave the solution for this problem and for situations with different boundary conditions, but did not investigate further. Jaeger [6] appears to have been the first to examine the integral in (1.4), and gave the asymptotic behaviour $I \sim 1/(\ln t - 2\gamma)$ in order to calculate the heat flux from the inner boundary. This is referred to in Ritchie & Sakakura [7] and also in Carslaw & Jaeger [8, § 13.5].

We may also consider the similar problem of the temporal evolution of the solution to the Schrödinger equation in two dimensions outside a circular potential barrier at $r = a$. The governing equation is then

$$\mathrm{i}\hbar\frac{\partial\psi}{\partial t} = -\frac{\hbar^2}{2m}\nabla^2\psi \tag{1.8}$$

in the region $r > a$, with $\psi = 0$ on $r = a$. We shall take the initial condition $\psi = -V$ at $t = 0$, which is physically unrealistic. However other physical systems exhibiting the same asymptotic behaviour exist (e.g. Llewellyn Smith [9]). A straightforward change of variable enables this problem to be recast as the diffusion problem above: we write

$\psi = V + v_S$ and define a diffusion-like coefficient $\kappa_S = \hbar/2m$. The resulting equation is

$$\frac{\partial v_S}{\partial t} = \mathrm{i}\kappa_S \nabla^2 v_S, \tag{1.9}$$

with $v_S = V$ on $r = a$ and $v_S = 0$ at $t = 0$. This is the same as (1.1) with imaginary diffusion or equivalently imaginary time. We can formally find the solutions of this equations merely by replacing t by $\mathrm{i}t$ in all solutions.

We are thus led to the following questions. What is the large-time behaviour of the solution to this diffusion problem (1.1) and to the Schrödinger equation (1.8)? What are the asymptotic solutions in the regions and how do they differ in the regions $qr \ll 1$ and $qr = O(1)$?

These questions involve Ramanujan's integral for real and imaginary values, and its behaviour for large absolute values of its argument. The relevant asymptotic expansions are calculated in § 2. The numerical calculation of Ramanujan's integral for all arguments, along with the appropriate definition of the analytic continuation of Ramanujan's integral, is discussed in § 3. The relationship between the near and far fields is analysed in § 4. Finally, the results are summarised and discussed in § 5.

Finally, a brief note about the aim of this paper might be appropriate. Ramanujan's integral occurs in a variety of quite disparate contexts (see [9–12]), among others), but the most accessible reference, namely the Bateman Manuscript Project [13], contains some inaccuracies. In addition, the published literature concerning the asymptotic behaviour consists of a large number of unrelated strands. It seems appropriate to synthesise previous work in one place, in particular the extension to the complex plane which has not been extensively discussed. In addition, the canonical problem introduced above gives some insight into the limitations of the behaviour obtained from Ramanujan's integral.

2 Ramanujan's integral

2.1 Definition and properties

The definition (1.7) of Ramanujan's integral is due to Hardy [14]. The integral in this definition exists for all x in the complex right half-plane including the imaginary axis, and $N(x)$ is analytic in the open right half-plane. For later use, it will be convenient to take the branch of the logarithm with $-\pi < \arg x \leqslant \pi$.

Hardy was discussing an interpolation formula used in Ramanujan's flawed proof of the prime number conjecture, which in a special case reduces to the following relation:

$$v(x) = \mathrm{e}^x - \int_0^\infty \frac{\mathrm{e}^{-ux}}{\pi^2 + (\ln u)^2} \frac{\mathrm{d}u}{u} = \mathrm{e}^x - N(x), \tag{2.1}$$

where the special function $v(x)$ is defined by

$$v(x) \equiv \int_0^\infty \frac{x^u}{\Gamma(u+1)} \, \mathrm{d}u. \tag{2.2}$$

The function $v(x)$ was introduced by Volterra to solve integral equations with logarithmic kernels (cf. Volterra & Pérès [15]). From the definition (2.2), $v(x)$ is an analytic function defined in the cut complex x-plane. The Laplace transform of $v(x)$ is

$$\overline{v}(s) = \frac{1}{s \ln s}. \tag{2.3}$$

The derivation of (2.3) is formally valid for Re $s > 1$, but the function $\overline{v}(s)$ may be extended over the cut complex s-plane by analytic continuation. Using Bromwich's integral to invert (2.3) gives (2.1). We now investigate the behaviour of $N(x)$, initially for large positive x, and then for complex x with $|x|$ large.

2.2 Behaviour of Ramanujan's integral for large $|x|$

The large real-x limit has been investigated independently on several occasions. The Bateman Manuscript Project [13] gives an erroneous result based on the correct work of Ford [16]. This was pointed out later and the correct result was given by Dorning *et al.* [17]. A new and very elegant proof was then given by Bouwkamp [18], and this is referred to in Bleistein & Handelsmann [19]. Independently and earlier, a different proof had been given by Spencer & Fano [20]. This work was generalised by the results of Ritchie & Sakakura [7], which are mentioned in Carslaw & Jaeger [8]. Another primary source is Jaeger [6], who writes down the inverse logarithmic decay but does not motivate it. A final line of work is that of Hull & Froese [21], Wyman & Wong [22] and Riekstiņš [23] mentioned in Olver [24, Chap. 8, § 11.4], where the result is derived using Haar's method; Bender & Orszag [25] is similar.

The most elegant approach here is probably that of Bouwkamp [18], who treated the more general integral

$$F(x, a, \sigma) = \int_0^\infty \frac{u^{\sigma-1} \mathrm{e}^{-ux}}{a^2 + (\ln u)^2} \, \mathrm{d}u. \tag{2.4}$$

Thus $N(x) = F(x, \pi, 0)$. Consider the function

$$g(s) = -\frac{1}{a} \mathrm{e}^{\mathrm{i}as} \int_0^\infty \frac{u^{s+\sigma-1} \mathrm{e}^{-ux}}{\mathrm{i}a + \ln u} \, \mathrm{d}u \tag{2.5}$$

with the property that $F(x, a, \sigma) = \mathrm{Im}\, g(0)$. Then

$$\frac{\mathrm{d}g}{\mathrm{d}s} = -\frac{1}{a} \mathrm{e}^{\mathrm{i}as} \int_0^\infty u^{s+\sigma-1} \mathrm{e}^{-ux} \, \mathrm{d}u = -\frac{1}{a} \mathrm{e}^{\mathrm{i}as} \frac{\Gamma(s+\sigma)}{x^{s+\sigma}}. \tag{2.6}$$

Hence

$$g(0) = \frac{1}{a} \int_0^s \mathrm{e}^{\mathrm{i}av} \frac{\Gamma(v+\sigma)}{x^{v+\sigma}} \, \mathrm{d}v + g(s). \tag{2.7}$$

The crucial part of Bouwkamp's argument consists in bounding $g(s)$. This is possible for non-zero a, in which case

$$|g(s)| \leqslant \frac{1}{a} \int_0^s \frac{u^{s+\sigma-1} \mathrm{e}^{-ux}}{[a^2 + (\ln u)^2]^{1/2}} \, \mathrm{d}u < \frac{1}{a^2} \frac{\Gamma(s+\sigma)}{x^{s+\sigma}}. \tag{2.8}$$

Combining (2.4), (2.6) and (2.8) leads to the result

$$F(x, a, \sigma) = x^{-\sigma} \int_0^s \frac{\sin av}{a} \Gamma(\sigma + v) \mathrm{e}^{-v \ln x} \, \mathrm{d}v + \frac{K}{a^2} \frac{\Gamma(s+\sigma)}{x^{s+\sigma}}, \tag{2.9}$$

where $|K| \leqslant 1$. The relation (2.9) holds for $s \geqslant 0$ and $\sigma \geqslant 0$ (the case $\sigma = 0$ follows by continuity arguments). The integral on the right-hand side of (2.9) is a Laplace integral, while the second term is formally of smaller order for all s. Therefore, as $x \to \infty$,

$$F(x, a, \sigma) \sim x^{-\sigma} \sum_{n=0}^{\infty} \varphi_n(a, \sigma)(\ln x)^{-n-1}, \tag{2.10}$$

where

$$\frac{\sin ax}{a} \Gamma(\sigma + x) \equiv \sum_{n=0}^{\infty} \varphi_n(a, \sigma) \frac{x^n}{n!}. \tag{2.11}$$

There may also be 'algebraically small terms' in the expansion, of order x^{-1}, but they cannot be obtained using this method.

For Ramanujan's integral, the expansion (2.10) becomes

$$N(x) \sim \sum_{k=0}^{\infty} \frac{(-1)^k c_{k+1} k!}{(\ln x)^{k+1}}, \tag{2.12}$$

where the c_k are defined by the generating function [26]

$$\sum_{k=1}^{\infty} c_k z^k \equiv \frac{1}{\Gamma(z)} = z + \gamma z^2 + \left(\frac{\gamma^2}{2} - \frac{\pi^2}{12}\right) z^3 + \cdots. \tag{2.13}$$

Therefore

$$N(x) \sim \frac{1}{\ln x} - \frac{\gamma}{(\ln x)^2} + \frac{\gamma^2 - \frac{\pi^2}{6}}{(\ln x)^3} + O\left(\frac{1}{(\ln x)^4}\right). \tag{2.14}$$

Bouwkamp's expansion (2.10) was derived under the assumption that x is real, and the relation $N(x) = F(x, \pi, 0)$ only holds when this is the case. However, an expansion valid in the closed right-half plane, where the integral definition of $N(x)$ is valid, may be derived by a similar procedure. This range is sufficient to obtain results for the Schrödinger equation where x is imaginary. Writing $x = \rho e^{i\theta}$, $N(x)$ becomes

$$N(\rho e^{i\theta}) = \int_0^{\infty} \frac{e^{-v\rho}}{\pi^2 + (\ln v - i\theta)^2} \frac{dv}{v}, \tag{2.15}$$

where this expression holds for $-\frac{\pi}{2} \leqslant \theta \leqslant \frac{\pi}{2}$. The path of integration has been rotated in the complex v-plane back onto the real axis, which is permissible for this range of θ because the integrand has no singularities in the right half of the v-plane. The integrand (2.15) can be decomposed using partial fractions, giving

$$N(\rho e^{i\theta}) = \int_0^{\infty} \frac{e^{-v\rho}}{2\pi i} \frac{dv}{v} \left[\frac{1}{\ln v - i\theta - i\pi} - \frac{1}{\ln v - i\theta + i\pi}\right]. \tag{2.16}$$

Now ρ is real and Bouwkamp's result can be extended by considering the function

$$h(s) = \frac{1}{2\pi i} \left[e^{-i(\theta+\pi)s} \int_0^{\infty} \frac{u^{s+\sigma-1} e^{-u\rho}}{\ln u - i\theta - i\pi} du - e^{-i(\theta-\pi)s} \int_0^{\infty} \frac{u^{s+\sigma-1} e^{-u\rho}}{\ln u - i\theta + i\pi} du\right]. \tag{2.17}$$

Then

$$\frac{dh}{ds} = \frac{1}{\pi} e^{-i\theta s} \sin \pi s \frac{\Gamma(s+\sigma)}{\rho^{s+\sigma}} = \frac{1}{\pi \rho^{\sigma}} \sin \pi s \frac{\Gamma(s+\sigma)}{x^s}. \tag{2.18}$$

Therefore

$$h(0) = \frac{1}{\pi\rho^{\sigma}} \int_0^s \sin \pi v \frac{\Gamma(v+\sigma)}{x^v} \, \mathrm{d}v + h(s) = \frac{1}{\pi} \int_0^s \mathrm{e}^{-\mathrm{i}\theta v} \sin \pi v \frac{\Gamma(v+\sigma)}{\rho^{v+\sigma}} \, \mathrm{d}v + h(s). \quad (2.19)$$

It is possible to bound $h(s)$, since

$$|h(s)| \leqslant \frac{1}{2\pi} \left[\frac{1}{|\pi+\theta|} + \frac{1}{|\pi-\theta|} \right] \frac{\Gamma(s+\sigma)}{\rho^{s+\sigma}}, \quad (2.20)$$

which is bounded for the range of θ under consideration. Taking the limit $\sigma \to 0^+$ as before leads to the two asymptotic expansions

$$N(x) \sim \sum_{k=0}^{\infty} \frac{(-1)^k c_{k+1} k!}{(\ln x)^{k+1}}, \quad (2.21)$$

$$N(\rho \mathrm{e}^{\mathrm{i}\theta}) \sim \sum_{n=0}^{\infty} \frac{\psi_n(\theta)}{(\ln \rho)^{n+1}}, \quad (2.22)$$

with the new generating function for the second expansion

$$\mathrm{e}^{-\mathrm{i}\theta x} \frac{\sin \pi x}{\pi} \Gamma(x) \equiv \sum_{n=0}^{\infty} \psi_n(\theta) \frac{x^n}{n!}. \quad (2.23)$$

Both expansions hold in the closed right-half plane. The first expansion, which is the same as for real x, is in terms of the gauge functions $\phi_n \equiv (\ln x)^{-n}$, while the second one is in terms of the gauge functions $(\ln |x|)^{-n}$. Similar results were obtained by Wyman & Wong [22].

The question of which asymptotic series represents the behaviour of $N(x)$ more efficiently off the real axis recalls problems in matched asymptotic expansions concerned with optimal inverse-logarithmic gauge functions (cf. Crighton & Leppington [27]). However, it is clear that

$$\left| \frac{\phi_{n+1}}{\phi_n} \right| = \left| \frac{1}{\mathrm{i}\theta + \ln \rho} \right| \leqslant \frac{1}{|\ln \rho|}. \quad (2.24)$$

This shows that the ratio of successive asymptotic gauge functions decreases faster off the real axis than on it, and one would expect the expansion (2.21) to do a better job than (2.22). One good reason to prefer the expansion in $(\ln x)^{-1}$ is that it can hence represent the behaviour of $N(x)$ for x with nonzero real part with one term.

2.3 Behaviour of $N(x)$ for small $|x|$

This expansion was first discussed in Volterra & Pérès [15]. It is outlined in the Bateman Manuscript Project [13] and set as exercise in Olver [24]. It is not physically relevant, but is included for completeness. The behaviour of $N(x)$ close to the origin is obscure when starting from (1.7). However, the relation (2.1) gives a simple way to compute the desired asymptotic expansion. Following Olver [24, Chap. 3, Ex. 8.6], we may apply Watson's lemma to (2.2) to obtain

$$v(x) \sim \sum_{n=0}^{\infty} c_{n+1} n! \, (\ln \tfrac{1}{x})^{-n-1}. \quad (2.25)$$

The behaviour of $N(x)$ now follows very simply as

$$N(x) \sim 1 - \frac{1}{\ln \frac{1}{x}} - \frac{\gamma}{(\ln \frac{1}{x})^2} - \frac{\gamma^2 - \frac{\pi^2}{6}}{(\ln \frac{1}{x})^3} + O\left(\frac{1}{(\ln \frac{1}{x})^4}\right). \tag{2.26}$$

This derivation is valid for $|\arg \ln \frac{1}{x}| < \pi$. Certainly for large enough x, it holds in the cut complex plane. It is also possible to obtain an expansion in $(\ln \rho)^{-1}$ where $\rho = |x|$ again, from the integral representation

$$v(\rho e^{i\theta}) = e^{-i\theta} \int_0^\infty \frac{e^{-v \ln \frac{1}{\rho}}}{\Gamma(v e^{-i\theta} + 1)}\, dv. \tag{2.27}$$

The resulting expansion is

$$N(\rho e^{i\theta}) \sim \sum_{n=0}^{\infty} e^{-i(n+1)\theta} \frac{c_{n+1} n!}{(\ln \frac{1}{\rho})^{n+1}}. \tag{2.28}$$

As in the case of the large-$|x|$ expansion, the form (2.26) is the more efficient, certainly in the sense of giving the better approximation with two terms. It is interesting to note that, apart from the constant term, (2.26) is the negative of (2.14).

3 Analytic continuation and numerical calculation of Ramanujan's integral

The integral (2.15) is equal to the definition (1.7) where the latter exists. However, (2.15) exists over the cut complex plane, so it is the analytic continuation of (1.7) beyond its domain of definition and we may use it to define Ramanujan's integral over the cut complex plane. This shows immediately that the expansions (2.21) and (2.22) are valid over the cut complex plane.

The analytic continuation can also be achieved by using the relation (2.1) to define $N(x)$ in the left half-plane. This is equivalent to defining $N(x)$ in the left half-plane by analytic continuation of its Laplace transform

$$\overline{N}(s) = -\frac{1}{s \ln s} + \frac{1}{s-1} \tag{3.1}$$

to $\operatorname{Re} s < 1$.

We are now in a position to compute Ramanujan's function over the complex plane. Dorning, Nicolaenko & Thurber [17] computed $N(x)$ numerically for real x to examine the accuracy of the asymptotic formula (2.12), using the formula

$$N(x) = \frac{1}{\pi} \int_{-\pi/2}^{\pi/2} e^{-x \exp(-\pi \tan v)}\, dv. \tag{3.2}$$

Here, however, we use the representation of $N(x)$ as an inverse Laplace transform to compute $N(x)$ for real x in a very efficient manner, using Talbot's algorithm [28] applied to (3.1). The function $\overline{N}(s)$ has no poles in the complex s-plane, and a branch cut along the negative real axis. Figure 1 shows a plot of $N(x)$ for real positive x computed using Talbot's algorithm, as well as the small-x and large-x asymptotic approximations. Talbot's algorithm is more efficient than the numerical computation of (3.2): to obtain 15 digit accuracy, the number of functional evaluations of $\overline{N}(s)$ is 28 for each point, whatever

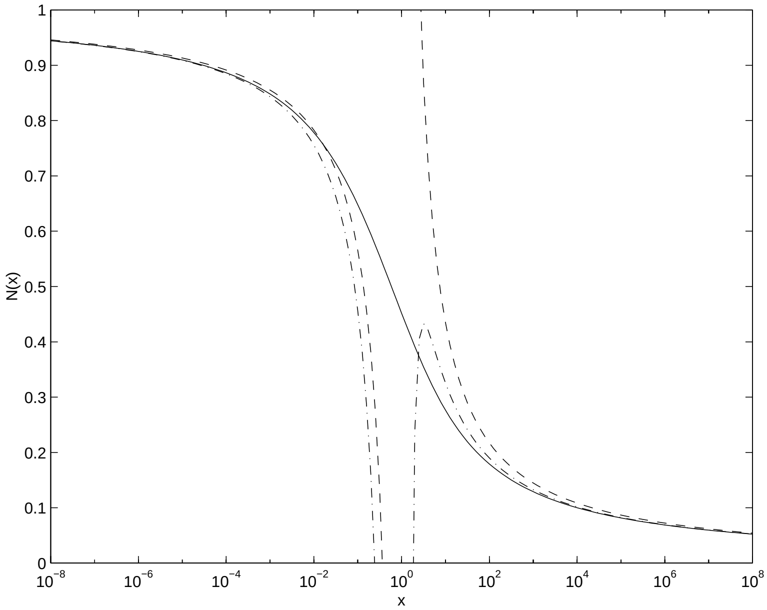

FIGURE 1. Plot of $N(x)$ against x. The solid curve is $N(x)$. The dash-dot curves show $1+(\ln x)^{-1}-\gamma/(\ln x)^{-2}$ for $x<1$ and $(\ln x)^{-1}-\gamma/(\ln x)^{-2}$ for $x>1$. The dashed curves show these expressions truncated one term earlier.

the value of x. The results of Talbot's algorithm were compared with the numerical integration of (3.2) using the routine DQAG with 12 digit relative accuracy and the results agree to 15 decimal places; this requires as many as 710 functional evaluations, a factor of 25 times more than Talbot's algorithm.

To calculate $N(x)$ for complex values of x, we could try to use Talbot's algorithm by considering the Laplace transform of $N(\rho e^{i\theta})$ as a function of the real variable ρ,

$$\int_0^\infty N(e^{i\theta}\rho)e^{-s\rho}\,d\rho = e^{-i\theta}\overline{N}(e^{-i\theta}s), \tag{3.3}$$

where the contour of integration has been rotated back onto the real axis, which is permissible for $-\frac{\pi}{2} \leqslant \theta \leqslant \frac{\pi}{2}$. However, the resulting algorithm does not converge off the real axis. The error is negligible for $\theta = \frac{\pi}{4}$ but subsequently grows rapidly, limiting the procedure to one significant figure on the imaginary axis.

The integral (3.2) does not converge in the left half-plane, and becomes numerically awkward close to the imaginary axis. We therefore use an alternative strategy. We calculate the integral in (3.2) between the limits $-\tan^{-1}(\frac{1}{\pi}\ln l)$ and $\frac{\pi}{2}$, and then integrate (2.15) from $le^{i\theta}$ to l and from l to ∞. The resulting sum gives $N(x)$ at any point in the complex plane. The advantage of this somewhat laborious technique is that it entails the integration of non-singular functions over finite regions on the first two contours, again carried out using DQAG, and the integration of an exponentially decaying function at infinity, carried out using DQAGIE. Other approaches also work, naturally.

Figure 2 shows $N(x)$ calculated in this way for $\theta = \frac{\pi}{4}$. This result was compared with (3.2) in the open right half-plane, and the results agreed to 15 significant figures. The

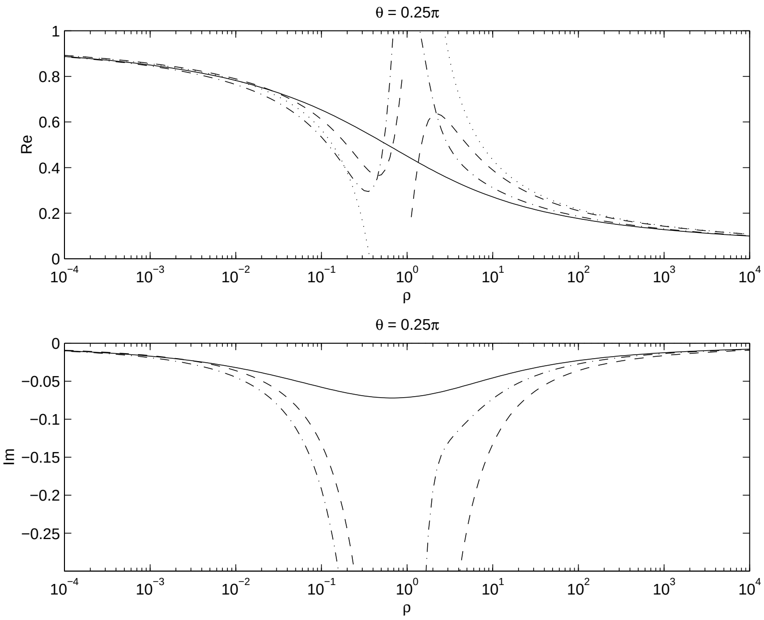

FIGURE 2. Plot of the real and imaginary parts of $N(x)$ against $\rho = |x|$ for $\arg x = \frac{\pi}{4}$. The dashed and dash-dot curves are as in Figure 1. The heavy dots show $(\ln|x|)^{-1}$ for $|x| > 1$ and $1 + (\ln|x|)^{-1}$ for $|x| < 1$.

range is smaller than in Figure 1 to show the detail in the transition region where the imaginary part is greatest in modulus. The real part of $N(x)$ in Figure 2 resembles the case for real x very closely. The imaginary part is always negative and has a minimum of -0.072 around $\rho = 0.676$.

The corresponding graphs for $\theta = \frac{\pi}{2}$, which corresponds to Schrödinger's equation, is shown in Figure 3. The curves are very similar to those of Figure 2. The minimum value of the imaginary part is now -0.150, attained at $|x| = 0.708$. The numerical evaluation of these curves took up to 50,000 functional evaluations to obtain 12 digit accuracy: the procedure is much less efficient than the case of real x.

Figure 4 shows an example of Ramanujan's integral in the left half-plane, for the case $\theta = \frac{3\pi}{4}$. Again, the curves are very similar to those in the rest of the complex plane, albeit the imaginary part is greater and the real part decreases slightly more steeply. The minimum value of the imaginary part is -0.245, taken at $\rho = 0.759$.

4 Near and far field behaviour of the diffusion equation

The asymptotic behaviour derived for the diffusion equation (1.1) is

$$v = V + 2V \ln(r/a)\left(\frac{1}{\ln \tau} + \cdots\right) + \cdots, \tag{4.1}$$

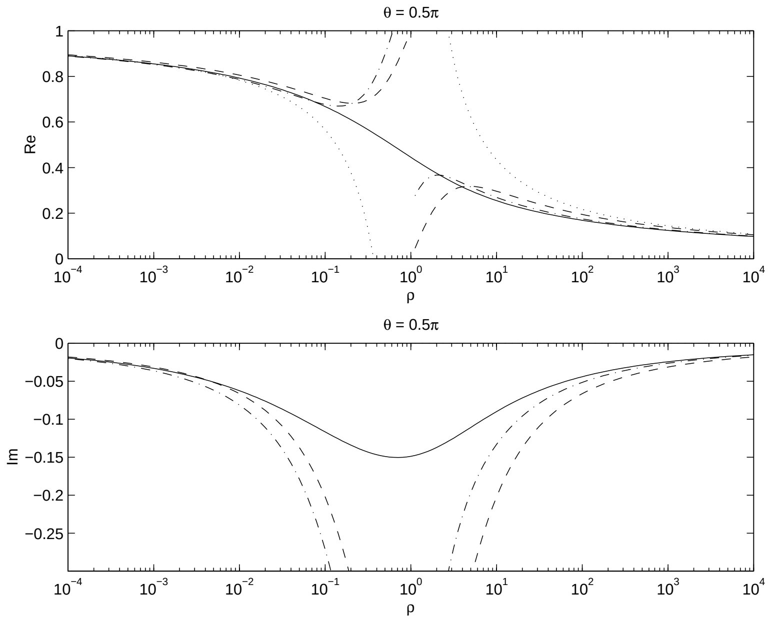

FIGURE 3. Plot of the real and imaginary parts of $N(x)$ against $\rho = |x|$ for $\arg x = \frac{\pi}{2}$. The curves are as in Figure 2. The phase of x corresponds to Schrödinger's equation.

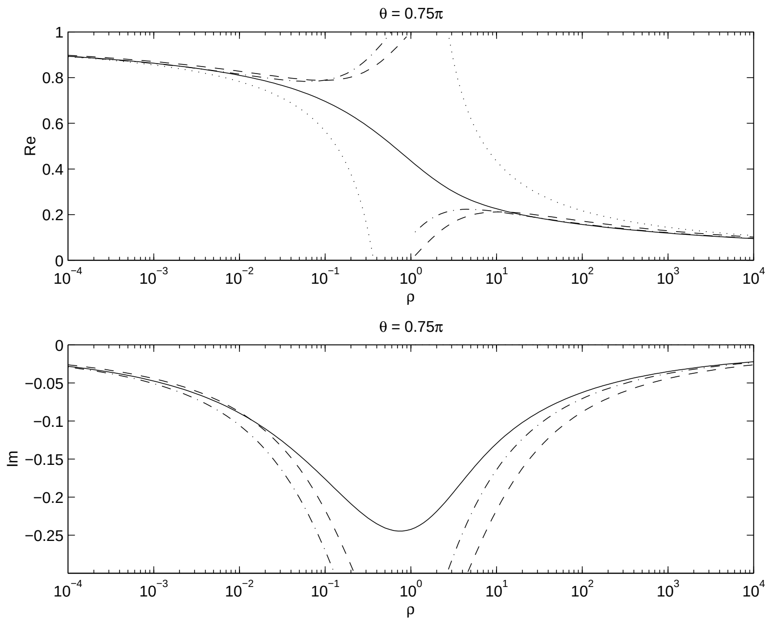

FIGURE 4. Plot of the real and imaginary parts of $N(x)$ against $\rho = |x|$ for $\arg x = \frac{3\pi}{4}$. The curves are as in Figure 2.

which cannot hold for large r. The appropriate expansion in the Laplace variable, corresponding to $qr = O(1)$, is

$$\bar{v} = -\frac{2VK_0(qr)}{s\ln(sa^2e^{2\gamma}/4\kappa)} + O(1). \tag{4.2}$$

The Bessel function in (4.2) can be related to the Laplace transform in time of the causal Green's function for the heat equation in two dimensions. We define the latter to be the solution of

$$\frac{\partial g}{\partial t} = \kappa\nabla^2 g + \delta(t)\delta(\mathbf{x}). \tag{4.3}$$

The Laplace transform of g is therefore given by

$$\bar{g} = \frac{K_0(qr)}{2\pi\kappa}, \tag{4.4}$$

which has the inverse transform

$$g = \frac{1}{4\pi\kappa t}e^{-\xi^2}H(t), \tag{4.5}$$

where $\xi = r/\sqrt{4\kappa t}$ is the usual similarity variable for the diffusion equation and H is the Heaviside step function. Therefore the solution (1.3) to the diffusion problem can be written as

$$v = g * \mathscr{L}^{-1}\left(\frac{2\pi\kappa V}{sK_0(qa)}\right), \tag{4.6}$$

where $\mathscr{L}^{-1}$ denotes the inverse Laplace transform and $*$ represents convolution in time. Inverting the expansion (4.2) shows that the solution for large t and r is approximated by

$$v \sim -g * \mathscr{L}^{-1}\left(\frac{4\pi\kappa V}{s\ln(sa^2e^{2\gamma}/4\kappa)}\right) = -4\pi\kappa V g * N(\tau). \tag{4.7}$$

Calculating the large-time behaviour of (4.7) requires dealing with the convolution in the time variable.

A more direct way of proceeding is to consider the initial problem again, armed with our knowledge of the asymptotic solution (4.1). The behaviour derived in § 1 has time dependence $(\ln\tau)^{-1}$. Therefore we seek an expansion in the form

$$v = \sum_{n=0}^{\infty}\frac{v_n(\xi)}{(\ln\tau)^{n+1}}. \tag{4.8}$$

Written in terms of τ and $\xi = r/\sqrt{4\kappa t}$, the diffusion equation (1.1) becomes

$$4\tau\frac{\partial v}{\partial \tau} = \frac{\partial^2 v}{\partial \xi^2} + \left(\frac{1}{\xi} + 2\xi\right)\frac{\partial v}{\partial \xi}. \tag{4.9}$$

On substituting (4.8) into (4.9), the leading-order τ derivative cancels, showing that the dominant far-field solution, apart from the inverse logarithm term, depends only on the similarity variable. The governing equation at leading order is

$$v_0'' + \left(\frac{1}{\xi} + 2\xi\right)v_0' = 0, \tag{4.10}$$

and the solution that decays at infinity is

$$v_0 = AE_1(\xi^2), \tag{4.11}$$

where E_1 is the exponential integral [26]. The unknown coefficient A in (4.11) must be determined through matching with (4.1). The small-ξ behaviour of (4.11) is

$$v_0 = A(-\gamma - 2\ln\xi + O(\xi^2)), \tag{4.12}$$

which leads to the final answer

$$v = \frac{VE_1(\xi^2)}{\ln\tau} + O\left(\frac{1}{(\ln\tau)^2}\right) \tag{4.13}$$

for $\tau \gg 1$ and $\xi \geqslant O(1)$. The match is carried out using an intermediate variable and the relation $\xi = r\mathrm{e}^{-\gamma}/(a\sqrt{\tau})$: the constant term is matched to give $A = V$. The approximate solution (4.13) corresponds in effect to the first term in the expansion of (4.7) in $(\ln\tau)^{-1}$.

The derivation of (4.13) is analytically easier than calculating the asymptotic behaviour of (4.7). The case of the Schrödinger equation differs only by a change of phase in the argument of the exponential integral (cf. Llewellyn Smith [9]).

We therefore have four different approximations to the exact solution $v(r,t)$: two for $r = O(1)$, namely the Ramanujan integral solution (1.6) and its expansion (4.1), and two for $\xi = O(1)$: the convolution (4.7) and the first term in its expansion in $(\ln\tau)^{-1}$, (4.13).

Figure 5 shows the solution $v(r,t)$ against radius r for $\tau = 50$ calculated using Talbot's algorithm, which was also used to calculate the inverse transform of (1.3). All results were calculated to 12 decimal places. The convolution (4.7) is a very good approximation to the exact solution over the whole of range of r shown and appears to satisfy the boundary condition on the cylinder. This is actually incorrect, but only by a factor of 0.03%. The expression (4.13) is a good approximation for $r > 5$ or so, but fails closer to the cylinder. The two inner expansions only agree very close to the cylinder: $N(\tau)$ provides a good approximation up to about $r = 4$, while the expansion (4.1) only seems accurate up to $r = 2$.

It is now worth considering the accuracy of the asymptotic expansions derived. The asymptotic expansions (1.6) and (4.1) are valid only near the cylinder. We may somewhat arbitrarily consider them to be good approximations when the relative difference from the exact answer is less than 1%, for example. Figure 6(a) shows the values of r/a at which the expansions become incorrect by a factor of 1%, plotted against the nondimensional time τ. The regions of validity grow very slowly away from the cylinder as τ increases in a parabolic fashion. This is natural since for constant ξ, $\tau \sim r^2$.

Determining the region where the outer solution is valid is more awkward. Examining the behaviour of the exact and approximate solutions shows that for large τ (say larger than 40), the difference between v and the far-field approximations is smaller than the value of v, at least while the latter is larger than the numerical precision attainable (12 decimal places). For larger r however, the numerical error becomes large. The quality of the approximations hence cannot be assessed in a convenient fashion. This behaviour cannot be seen in Figure 6(a), of course.

What may be estimated, however, is the accuracy of the approximate solutions on the boundary of the cylinder. For values of τ less than 8, both expansions are quite hopeless.

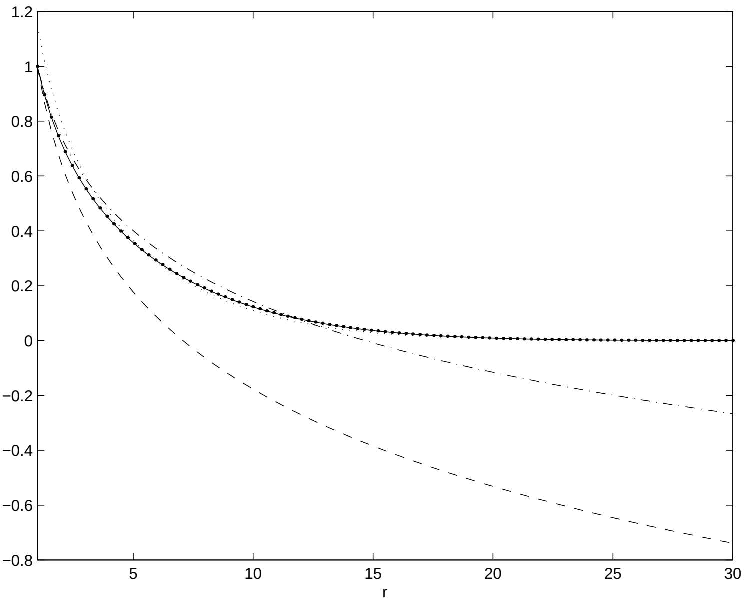

FIGURE 5. Exact and approximate solutions to the diffusion problem (1.1) for $a = 1$, $\kappa = \frac{1}{2}$ and $V = 1$ for $\tau = 50$ (corresponding to $t = 79.3$). The solid curve shows v. The dash-dot show the leading-order asymptotic expansion (i.e. Ramanujan's integral) close to the cylinder (1.6) and the dashed curve shows the first term in the inverse logarithmic expansion of Ramanujan's integral (4.1). The heavy dots show the convolution (4.7) and the light dots show the first term in the expansion (4.13).

For larger τ however, the values of (4.7) and (4.13) on the boundary are shown in figure 6(*b*). Both are good estimates. The behaviour of the leading-order term in the expansion (4.13) can be obtained analytically as

$$v(r = a) \sim \frac{VE_1(\mathrm{e}^{-2\gamma}/\tau)}{\ln \tau} + \cdots \sim V + \frac{V\gamma}{\ln \tau} + \cdots, \tag{4.14}$$

which approaches the correct boundary condition in an inverse logarithmic fashion.

5 Conclusion

The large-time asymptotic behaviour of the evolution of temperature around a constant-temperature cylinder in two dimensions leads naturally to Ramanujan's integral. We have reviewed the asymptotic behaviour of Ramanujan's integral for large real values of the argument as well as in the complex plane, which is relevant to the large-time behaviour of Schrödinger's equation in similar radial geometries. The general complex case requires the analytic continuation of Ramanujan's integral over the complex plane which can be accomplished using (2.15) or (3.1). The Stokes lines of the analytic continuation of Ramanujan's integral have not been discussed here, but they might be of some interest, even though the asymptotic decay is the same over the whole complex plane.

Ramanujan's integral may be calculated efficiently on the real axis from its Laplace transform using Talbot's algorithm. However, this procedure fails off the real axis where

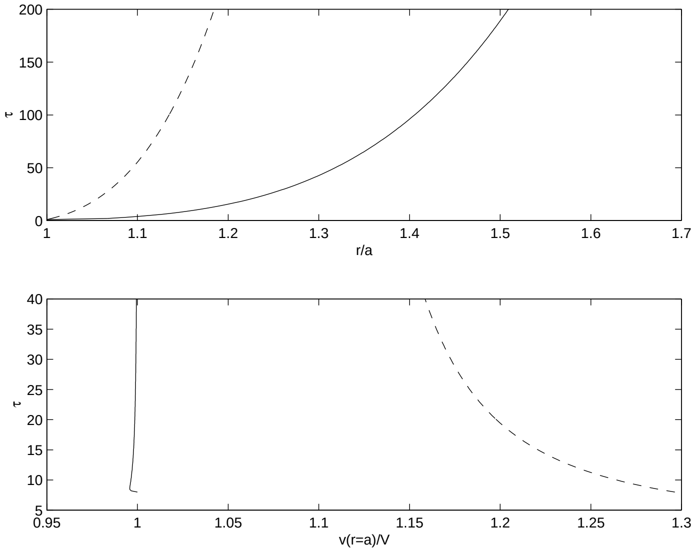

FIGURE 6. (*a*) Limits of regions of validity of the expansions (1.6) (solid curve) and (4.1) (dashed curve) plotted against τ on the vertical axis. (*b*) Value of v on the boundary of the cylinder for the convolution (4.7) (solid curve) and the first term in expansion (4.13) (dashed curve), again plotted against τ on the vertical axis.

Ramanujan's integral may be calculated using an integral representation valid over the whole complex plane. The failure of Talbot's algorithm is interesting and appears related to the displacement of the branch cut off the negative real axis as the argument of x changes; this leads to non-analyticity of the Laplace transform for arbitrarily large values of the imaginary part of s which seems to be enough to invalidate the partly empirical error bounds derived by Talbot.

For large values of time, the formal asymptotic solution (1.6) is not a good approximation far from the cylinder. This is evident from the non-uniformity in the Laplace variable of the expansion used to derive (1.6) for large r.

A solution valid far from the cylinder may be obtained in the form of a convolution, and may be calculated from its Laplace transform in an efficient manner. Once again, this solution may be expanded as an asymptotic series in inverse logarithmic powers of τ. An easy way of doing this is presented, using the method of matched asymptotic expansions. Far from the cylinder, the solution does not depend on the radius of the cylinder and the spatial dependence of the solution should be given by a function of the usual similarity variable ξ. What might be termed an intermediate asymptotic solution (cf. Barenblatt [29]) therefore holds in this region. The derivation by matched asymptotic expansions leads rapidly to a simple answer which is a very good approximation to the full convolution (4.7). Both the convolution solution and the similarity-type solution are very good approximations to the full solution over most of r, whereas the solution that is given by Ramanujan's integral does poorly.

As is evident from (1.5), the Laplace transform of Ramanujan's integral is related in a very simple fashion to the function $(\ln s)^{-1}$ and hence what we have examined is the behaviour of a prototypical function with inverse-logarithmic Laplace transform. The behaviour of Ramanujan's integral over the complex plane is rather dull and its real part in particular changes very little with the phase of its argument. However, at the branch cut along the negative real axis, there is a change of sign in a term subdominant to the expansions that were calculated.

The physical problem that was considered here is of course special in the sense that the solution can be written down and analysed in some detail. However, the features of its solution for large time should be characteristic of any diffusion problem with radial geometry, and the techniques used here can be extended to such problems.

Acknowledgements

The author was supported by a Research Fellowship from Queens' College, Cambridge. Discussions with Bill Young and Joe Keller were very helpful. Comments from anonymous referees and John Ockendon led to valuable improvements in the manuscript.

References

[1] Nicholson, J. W. (1921) A problem in the theory of heat conduction. *Proc. R. Soc. Lond.* A **100**, 226–240.
[2] Goldstein, S. (1932) Two-dimensional diffusion problems. *Proc. Lond. Math. Soc.* **34**, 51–88.
[3] Smith, L. P. (1937) Heat flow in an infinite solid bounded internally by a cylinder. *J. Appl. Phys.* **8**, 441–448.
[4] Carslaw, H. S. & Jaeger, J. C. (1940) Some problems in conduction of heat. *Proc. Lond. Math. Soc.* **46**, 361–388.
[5] Titchmarsh, E. C. (1948) *Introduction to the Theory of Fourier Integrals*. 2nd ed. Oxford University Press.
[6] Jaeger, J. C. (1941) Heat flow in the region bounded internally by a circular cylinder. *Proc. Roy. Soc. Edin.* A **61**, 223–228.
[7] Ritchie, R. H. & Sakakura, A. Y. (1956) Asymptotic expansions of solutions of the heat conduction equation in internally bounded cylindrical geometry. *J. Appl. Phys.* **27**, 1453–1459.
[8] Carslaw, H. S. & Jaeger, J. C. (1959) *Conduction of Heat in Solids*. 2nd ed. Oxford University Press.
[9] Llewellyn Smith, S. G. (1999) Near-inertial oscillations of a barotropic vortex: trapped modes and time evolution. *J. Phys. Oceanogr.* **29**, 747–761.
[10] Giles, M. J. (1995) Probability-distribution functions for Navier–Stokes turbulence. *Phys. Fluids* **7**, 2785–2795.
[11] Liu, Y. & Yue, D. K. P. (1996) On the time dependence of the wave resistance of a body accelerating from rest. *J. Fluid Mech.* **310**, 337–363.
[12] Taitelbaum, H. (1991) Nearest-neighbor distances at an imperfect trap in 2 dimensions. *Phys. Rev.* A **43**, 6592–6596.
[13] Bateman Manuscript Project (1955) *Higher Transcendental Functions*. McGraw-Hill.
[14] Hardy, G. H. (1940) *Ramanujan: Twelve Lectures on Subjects Suggested by his Life and Work*. Cambridge University Press.
[15] Volterra, V. & Pérès, J. (1924) *Leçons sur la Composition et les Fonctions Permutables*. Gauthier-Villars.
[16] Ford, W. B. (1936) *The Asymptotic Developments of Functions defined by MacLaurin Series*. University of Michigan Press.
[17] Dorning, J. J., Nicolaenko, B. & Thurber, J. K. (1969) An integral due to Ramanujan which occurs in neutron transport theory. *J. Math. Mech.* **19**, 429–438.

[18] Bouwkamp, C. J. (1971) Note on an asymptotic expansion. *Indiana U. Math. J.* **21**, 547–549.
[19] Bleistein, N. & Handelsman, R. A. (1986) *Asymptotic Expansions of Integrals*. Dover.
[20] Spencer, L. V. & Fano, U. (1954) Energy spectrum resulting from electron slowing down. *Phys. Rev.* **93**, 1172–1181.
[21] Hull, T. E. & Froese, C. (1955) Asymptotic behaviour of the inverse of a Laplace transform. *Canad. J. Math.* **7**, 116–125.
[22] Wyman, M. & Wong, R. (1969) The asymptotic behaviour of $\mu(z, \beta, \alpha)$. *Canad. J. Math.* **21**, 1013–1023.
[23] Riekstiņš, E. J. (1974) Asymptotic expansions for some types of integrals involving logarithms. *Latvii Mat. Ezegodnik* **15**, 113–130.
[24] Olver, F. W. J. (1974) *Asymptotics and Special Functions*. Academic.
[25] Bender, C. M. & Orszag, S. A. (1978) *Advanced Mathematical Methods for Scientists*. McGraw-Hill.
[26] Abramowitz, M. & Stegun, I. A. (1965) *Handbook of Mathematical Tables*. Dover.
[27] Crighton, D. G. & Leppington, F. G. (1973) Singular perturbation methods in acoustics: diffraction by a plate of finite thickness. *Proc. R. Soc. Lond.* A **335**, 313–339.
[28] Talbot, A. (1979) The accurate numerical inversion of Laplace transforms. *J. Inst. Math. Applic.* **23**, 97–120.
[29] Barenblatt, G. I. (1996) *Scaling, Self-similarity, and Intermediate Asymptotics*. Cambridge University Press.